

# Research into the relationship between the surface topography, texture and mechanical properties of PVD-Cu/Ni multilayers\*

B. KUCHARSKA<sup>1</sup>, E. KULEJ<sup>1†</sup>, G. PYKA<sup>2</sup>, J. KANAK<sup>3</sup>, T. STOBIECKI<sup>3</sup>

<sup>1</sup> Institute of Materials Engineering, Czestochowa University of Technology, al. Armii Krajowej 19, 42-200 Czestochowa

<sup>2</sup> Department of Metallurgy and Materials Engineering, Katholieke Universiteit Leuven, B-3001 Heverlee, Belgium

<sup>3</sup> Department of Electronics, AGH University of Science and Technology, 30 Mickiewicza Av., 30-059 Kraków

The paper presents the results of structural examinations and mechanical tests of Cu/Ni multilayers fabricated by the magnetron sputtering method. The investigated multilayers were differentiated by Ni sublayer thickness (1, 3 and 6 nm), while the retaining Cu sublayer thickness was unchanged (2 nm). Measurements demonstrated that the multilayers were strongly textured in the direction of their growth [111], with the thinnest multilayer (Cu/Ni = 2/1) showing a stronger texture. Stronger texturing was associated with greater surface roughness. Multilayers with the largest thickness had higher hardness and Young's modulus. The properties of Cu/Ni multilayers depended both on the thickness of their sublayers, as well as on their total thickness.

Keywords: *Cu/Ni multilayers; thermal stability; X-ray diffraction; texture; atomic force microscopy*

© Wrocław University of Technology.

## 1. Introduction

On a nanometric scale, multilayer coatings are characterized by unique mechanical and magnetic properties. Multilayers, in which ferromagnetic and diamagnetic material layers are laid alternately, have found application in electronics, *e.g.* for recording and reading heads and MRAM memory components [1, 2]. Moreover, these materials are distinguished by better mechanical properties, for instance, they have hardness values several times higher than that of solid materials, which allow them to be used in a number of potential applications in industry, from nano-devices to wear-resistance applications. They owe these unique properties to the existence of a distinct phase boundary. Its quality is determined primarily by very low roughness of the sublayers. The mechanical and magnetic properties are also significantly influenced by the conditions of fabrication, the microstructure, as well as the multilayer

texturing degree. The orientation of crystallites in a multilayer is dependent on many factors, including the type of materials used, and the thickness and arrangement sequence of the sublayers [3–11].

The aim of this study is to determine the correlation between the microstructure properties, *i.e.* texturing and roughness, and the mechanical properties (nanohardness and Young's modulus) of Cu/Ni with a differentiated Ni sublayer thickness.

## 2. Material and research methodology

Cu/Ni multilayers fabricated by the magnetron sputtering technique, deposited on a monocrystalline silicon substrate with the orientation (100), were investigated. The multilayers were built from 100 bilayers in which the Cu layer had an identical thickness of 2 nm, while the Ni layers differed in thickness that was 1, 3 and 6 nm, respectively. The list of sublayers thickness and total thickness of multilayers subjected to investigation is presented in Table 1.

\*This paper was presented at the 12<sup>th</sup> Seminar Surface and Thin-Film-Structures – SemPiSC, Szklarska Poręba 2012

†E-mail: kulej@wip.pcz.pl

Table 1. The sublayers and total thickness of the Cu/Ni multilayers.

Multilayer	Cu/Ni = 2/1	Cu/Ni = 2/3	Cu/Ni = 2/6
Cu sublayer thickness, nm	2	2	2
Ni sublayer thickness, nm	1	3	6
Bilayer thickness, nm	3	5	8
Total thickness, nm	300	500	800

The multilayers were subjected to X-ray, nanohardness and surface topography studies. The multilayer structure was measured using two X-ray diffractometers: powder Seifert 3003TT and X'Pert MPD and the wavelength of radiation generated by a copper anode tube ( $\lambda_{Cu} = 0.154$  nm). Measurements of  $\omega$  (rocking curve) were carried out and polar figures were plotted. The registration of the polar figures and the rocking curve measurements were made for the Cu/Ni(111) and Cu/Ni(200) reflections, while setting the position of the detector relative to the tube corresponding to the angles of  $43.5^\circ$  and  $50.4^\circ$ . The polar figures registration with the beam of radiation incident to the multilayer surface was collimated to a cross-section of  $\varnothing 2$  mm. The polar figures served for the calculation of the Orientation Distribution Function (ODF). Microhardness tests were performed by Berkovich's method using a CSM Nano/Micro-Hardness Tester with a load of 1 mN. For each sample, 5 measurements were taken, and the result was expressed as their arithmetic mean. The hardness of a multilayer was determined from the formula [12]:

$$H = \frac{F_{max}}{A} \quad (1)$$

where:  $F_{max}$  – maximum loading force,  $A$  – surface area of the contact between the indenter and the multilayer.

From the slope of the unloading curves, Young's modulus of the examined multilayers was determined using the equation below [13]:

$$\frac{1}{E_r} = \frac{1 - \nu_d^2}{E_d} + \frac{1 - \nu_m^2}{E_m} \quad (2)$$

where:  $E_d$  – Young's modulus of the diamond indenter (1141 GPa),  $\nu_d$  – Poisson's ratio of the diamond indenter (0.07),  $E_m$  – Young's modulus of the multilayer tested,  $\nu_m$  – Poisson's ratio of the multilayer tested (0.3),  $E_r$  – reduced Young's modulus:

$$E_r = \frac{1}{2\beta} \sqrt{\frac{\pi}{A_{(h_c)}}} \frac{dp}{dh} \quad (3)$$

where:  $\beta$  – coefficient resulting from the indenter geometry (1.012),  $A_{(h_c)}$  – indenter and multilayer contact surface area at the plastic indentation depth ( $h_c$ ),  $dp$  – force difference in the unloading curve in the maximum force range of 60 % ÷ 95 %,  $dp$  – indenter penetration depth difference in the maximum force range of 60 % ÷ 95 % in the unloading curve,  $dp/dh$  – quotient describing the rigidity of the material tested.

The surface topography of the multilayers was imaged using a Veeco atomic force microscope. The value of arithmetic mean roughness deviation,  $R_a$ , was calculated based on five randomly chosen areas (with a scanning area of  $16 \mu\text{m}^2$ ) using the Nanoscope software.

### 3. Results

#### 3.1. Multilayer texture

The polar figures originating from the planes Cu/Ni(111) and Cu/Ni(200) of the examined multilayers are shown in Fig. 1. The recorded distributions of poles on the polar figures indicate texturing of the planes in the multilayer growth direction. All of the presented Cu/Ni(111) and Cu/Ni(200) polar figures have a double symmetry, with the textures from the Cu/Ni(111) planes exhibiting a higher pole intensity compared to the Cu/Ni(200). The strongest Cu/Ni(111) texture is shown by the Cu/Ni = 2/1 multilayer, whereas in the case of the Cu/Ni(200) texture, by the Cu/Ni = 2/6 multilayer. The components of a multilayer (both Cu and Ni) have a face-centred cubic (fcc) lattice structure in which the closest packing of atoms occurs in its growth plane {111}. The strong texture of Cu/Ni multilayers in this plane is caused by the tendency of atoms to the densest filling of the space. The double symmetry of the figures is distinct in those multilayers

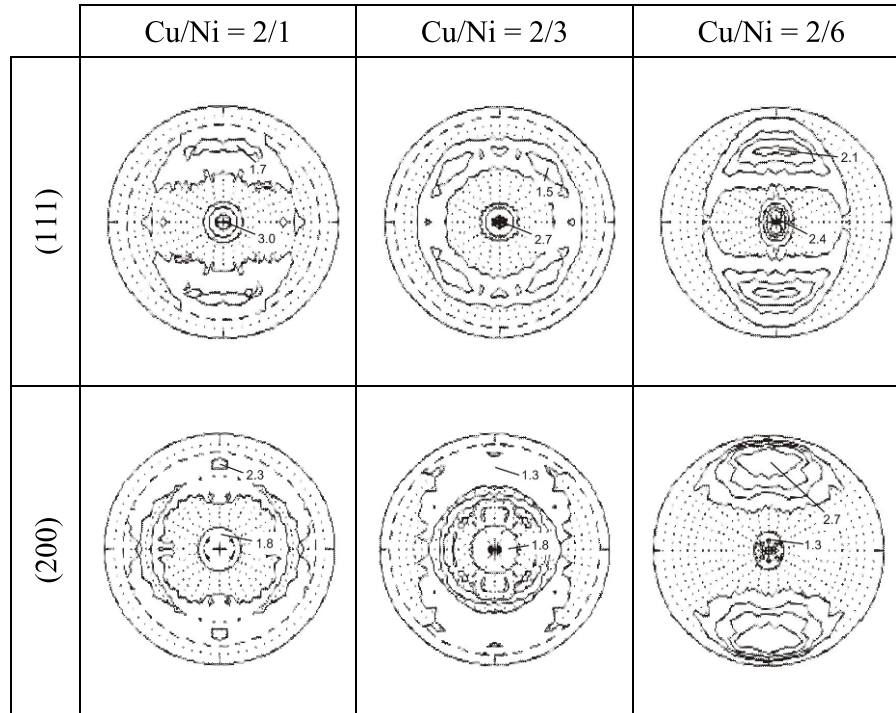


Fig. 1. Polar figures for the main reflections (111) and (200) of Cu/Ni multilayers.

in which the variation in multilayer thickness is the greatest. Considering the fact that multilayer deposition took place alternately from two targets situated at an angle relative to the substrate, it can be supposed that the polar figure symmetry is the result of a different particle flux originating from each of them. In the Cu/Ni = 2/3 multilayer, which has the layers of the closest thicknesses, the double symmetry effect is less distinctly marked. Indeed, in this case, the effect of particle flux magnitude is similar. In the Cu/Ni = 2/6 multilayer, the variation in the magnitudes of Cu and Ni atom flux is the greatest, therefore the double symmetry effect on the polar figures originating from this multilayer is the most distinct.

The outcome of the ODF analysis of texture measurements is shown in Fig. 2. Three fibres of the orientations  $\{665\}$ ,  $\{015\}$  and  $\{511\}$  can be distinguished in the Cu/Ni = 2/1 multilayer texture (Fig. 2a). The maximum value of the Orientation Distribution Function (ODF) for the Cu/Ni = 2/1 multilayer corresponds to the orientation  $\{015\}\langle 051\rangle$  and amounts to  $f(g) = 4.1$ . The fibre  $\{511\}$  has the strongest  $\{511\}\langle 194\rangle$

component, while the strongest component of the fibre  $\{655\}$  is  $f(g) = 3.2$  for the orientation  $\{655\}\langle 386\rangle$ .

The texture of the Cu/Ni = 2/6 multilayer, similarly as that of the thinnest multilayer Cu/Ni = 2/1, also has three fibres of the orientations  $\{511\}$ ,  $\{111\}$  and  $\{025\}$ , but they show lower ODF values. The highest Orientation Distribution Function value for this multilayer is  $f(g) = 3.0$  for the orientation  $\{511\}\langle 194\rangle$ , and a little lower value of  $f(g) = 2.7$  for the orientation  $\{025\}\langle 151\rangle$ . For the fibre  $\{111\}$ , the strongest orientation is  $\{111\}\langle 121\rangle$ .

The Cu/Ni = 2/3 multilayer has a fibrous structure, as evidenced both by the picture of the polar figures and by the Orientation Distribution Functions. A distinct single orientation  $\{229\}\langle 994\rangle$  occurs in the multilayer, for which the Orientation Distribution Function value amounts to  $f(g) = 2.9$ . In addition, also a relatively weak and broadened limited fibre  $\{110\}$  exists, in which two distinct orientations,  $\{111\}\langle 110\rangle$  and  $\{011\}\langle 111\rangle$ , occur. Two limited fibres of orientations  $\{111\}\langle 111\rangle$  and  $\{223\}\langle 692\rangle$  lie within the broadening of the  $\{111\}\langle uvw\rangle$  fibre.

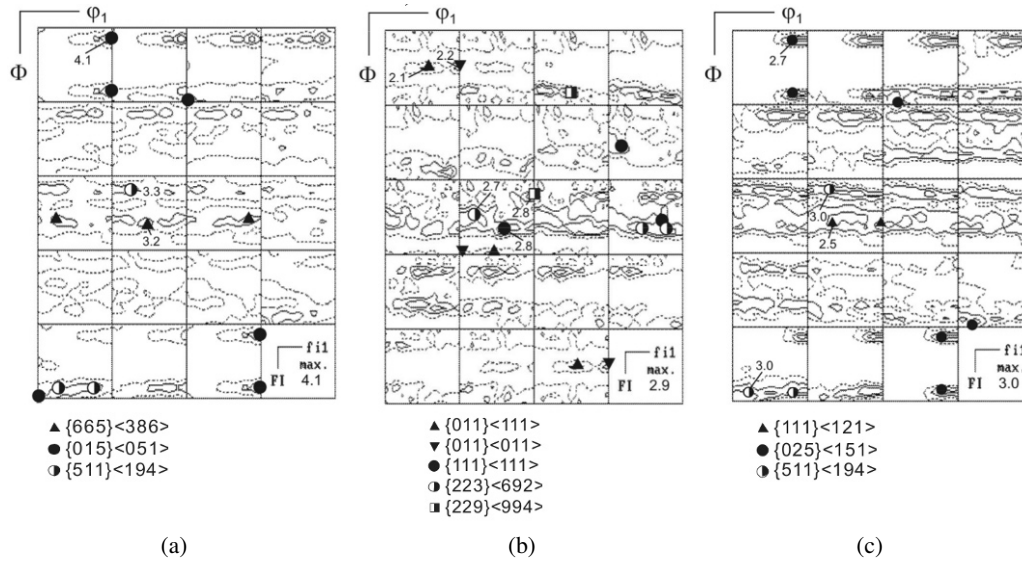


Fig. 2. Orientation Distribution Functions (ODF) for the Cu/Ni multilayer: a) Cu/Ni = 2/1, b) Cu/Ni = 2/3, Cu/Ni = 2/6.

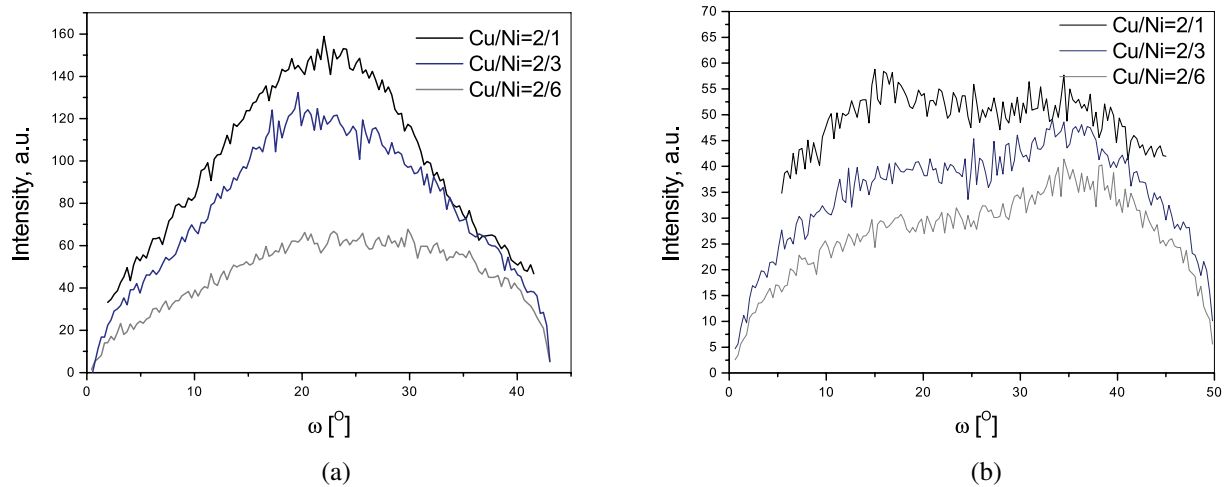


Fig. 3. Measurements of  $\omega$  for the Cu/Ni multilayer: a) for the Cu/Ni (111) reflection, b) for the Cu/Ni (200) reflection.

The planes  $\{025\}$  in the Cu/Ni = 2/6 multilayer form an angle of  $<1^\circ$  with the  $\{015\}$  planes in the Cu/Ni = 2/1 multilayer; however, the directions lying in these planes differ from one another.

The ODF analysis confirms the conclusions on the effect of variation of layer thickness on the multilayer texture, which resulted from the description of the polar figures.

The multilayer texture, illustrated also in the  $\omega$  measurements, is shown in Fig. 3. The rocking curve

shape confirms the conclusions derived from the preceding measurements. The curves for the multilayer with the highest layer thickness variation (Cu/Ni = 2/6) are the most asymmetric. For the description of the rocking curves, the half-widths of the reflections Cu/Ni(111) and Cu/Ni(200) were used. To determine the half-widths of the Cu/Ni(111) reflections, the diffraction curves were described with the Gaussian function (the fit example in Fig. 4). Due to their nature (a clear bifurcation and asymmetry of the

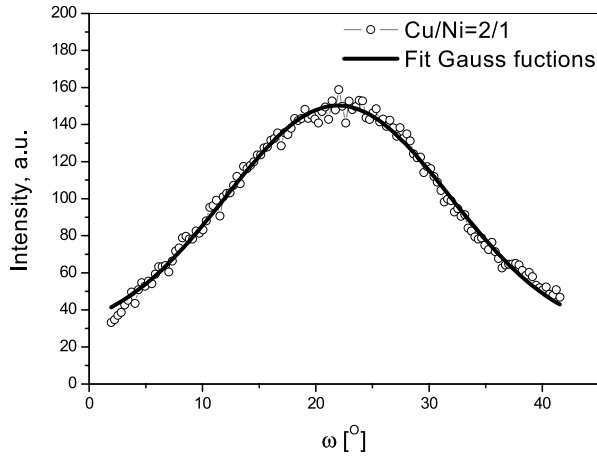


Fig. 4. Example of a Gaussian fit for the Cu/Ni = 2/1 multilayer and the (111) plane.

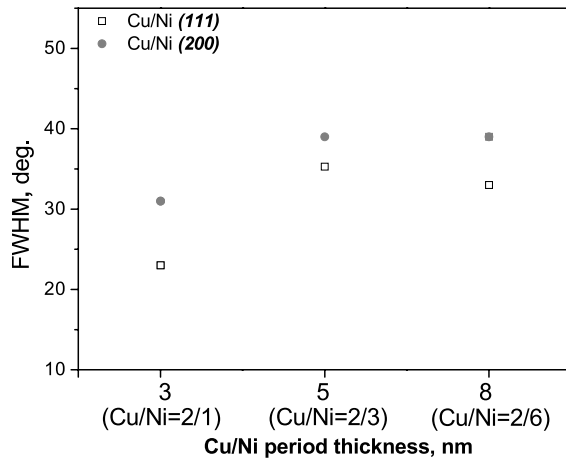


Fig. 5. Half-widths of the main X-ray reflections of Cu/Ni multilayers as a function of bilayers thickness.

peak top), the half-widths of the Cu/Ni(200) reflections were determined manually in the middle of their maximum intensity (Fig. 5).

The reflections coming from the Cu/Ni(111) planes have a smaller half-width and higher intensity, which confirms the view that the growth orientation [111] is predominant in all multilayers investigated. The Cu/Ni(200) reflections exhibit the weakest intensity and larger half-widths, which indicates a weaker multilayer texture in the [200] direction. The bifurcation of the Cu/Ni(200) reflection top is indicative of the absence of parallelism between this plane and the surface of the multilayers investigated.

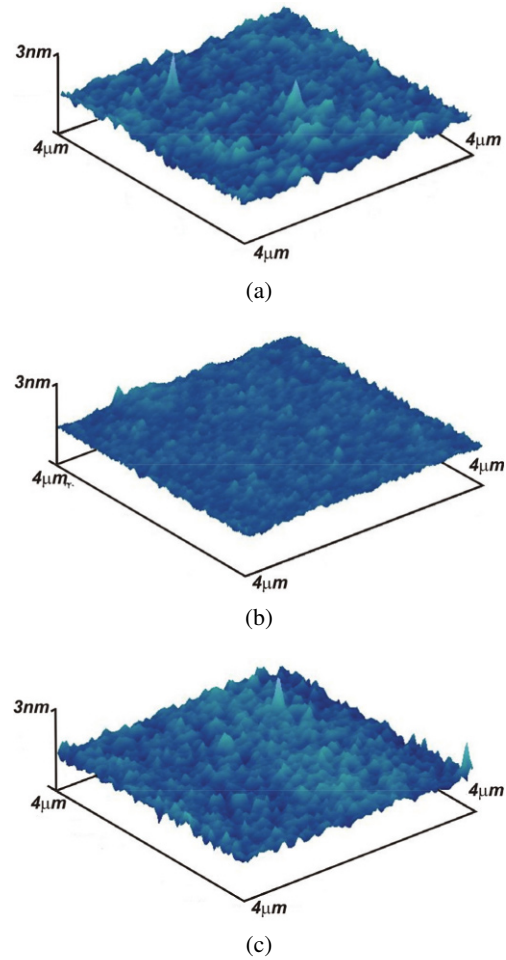


Fig. 6. AFM surface topography images for the multilayers: a) Cu/Ni = 2/1, b) Cu/Ni = 2/3, c) Cu/Ni = 2/6.

### 3.2. Multilayer surface topography

The multilayer surface topography, as obtained by the AFM method, is shown in Fig. 6. The Cu/Ni = 2/3 multilayer is characterized by the smallest surface development degree, and thus the lowest roughness. The most developed surface is exhibited by the multilayer with the thickest Ni sublayer (Cu/Ni = 2/6). For the Cu/Ni = 2/6 multilayer, the roughness value is comparable with the value determined for the thinnest multilayer. The values of Ra parameter for all multilayers are summarized in Table 2.

### 3.3. Multilayer hardness

The hardness tests showed that the Cu/Ni = 2/1 multilayer had the lowest hardness (3.52 GPa),

Table 2. A summary of the values of  $R_a$  roughness parameter for the multilayers investigated.

Multilayer	Cu/Ni = 2/1	Cu/Ni = 2/3	Cu/Ni = 2/6
$R_a$ , nm	0.34	0.17	0.36
Standard deviation, nm	$\pm 0.06$	$\pm 0.04$	$\pm 0.05$

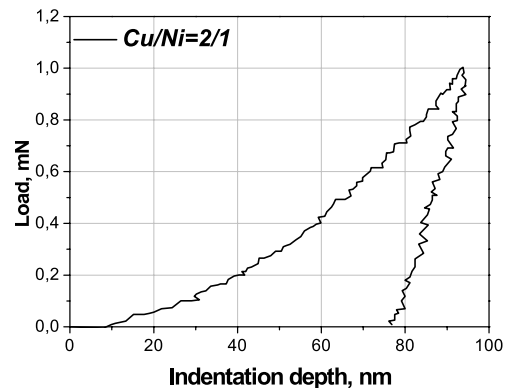
Table 3. The estimated number of bilayers covered by the nanohardness measurement carried out in a direct manner.

Multilayer	Cu/Ni = 2/1	Cu/Ni = 2/3	Cu/Ni = 2/6
Indenter penetration depth, nm	90	85	80
Number of bilayers covered by direct measurement	30	17	11
% of multilayer thickness covered by direct measurement	30	20	10
Hardness, GPa	3.52	4.68	7.20

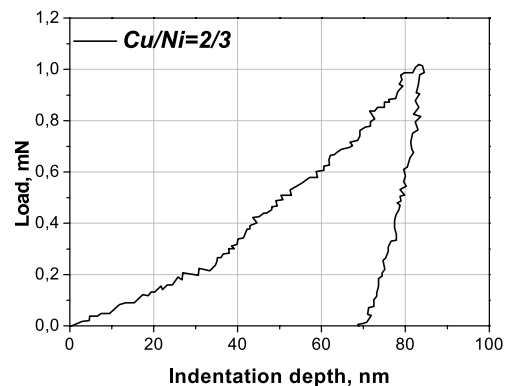
while the highest hardness (7.20 GPa) was exhibited by the Cu/Ni = 2/6 multilayer. In the examples of multilayer loading and unloading curves presented in Fig. 7 it is visible that with an identical maximum loading force of 1 mN being maintained for all multilayers, the indenter penetration depth into the thickest layer is the smallest.

Due to the differences in multilayer thickness and hardness, the measurements covered a different number of bilayers, which was determined based on the impression depth. The average indenter penetration into individual multilayers is given in Table 3. For the thinnest Cu/Ni = 2/1 multilayer, the direct measurement covered most of the bilayers (approx. 30 % of the multilayer). This means that this result might be burdened with the largest error resulting from the likely effect of the substrate on the measurement value.

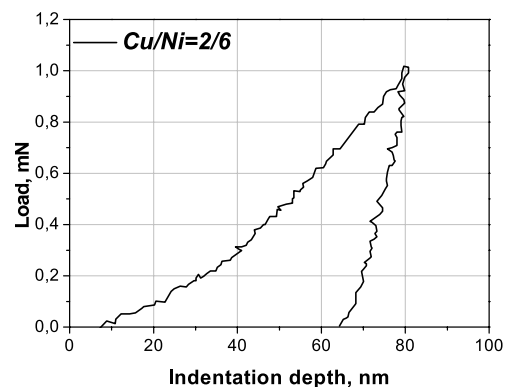
The hardness of the tested multilayers might also be affected by the share of the multilayer components. The hardness of the nickel layer deposited by the magnetron technique is higher compared to the Cu layer, as reported in the study by H.C. Barshilia



(a)



(b)



(c)

Fig. 7. Examples of Cu/Ni multilayer loading and unloading curves as a function of indenter penetration depth, a) Cu/Ni = 2/1, b) Cu/Ni = 2/6.

and K.S. Rajam [3] (see Fig. 8). Therefore, it can be presumed that increasing the Ni content in the Cu/Ni = 2/6 multilayer by six times compared to the Cu/Ni = 2/1 multilayer had also the effect on increasing the nanohardness value for this Cu/Ni multilayer.

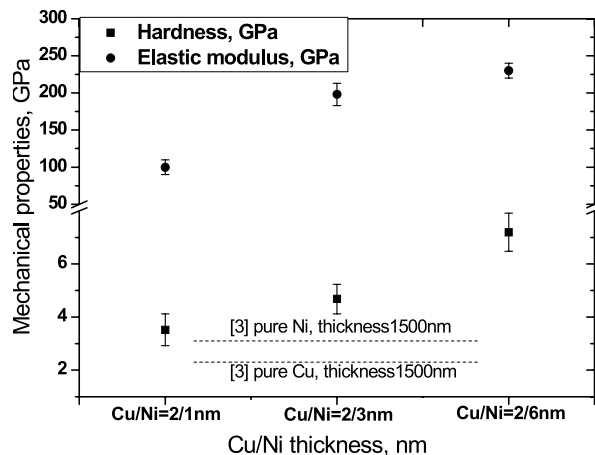


Fig. 8. Values of hardness and Young's modulus for Cu/Ni multilayers (the solid lines represent the hardness values of single Cu and Ni layers deposited by the magnetron technique – the results reported in reference [3]).

Based on the slope of the unloading curves, Young's moduli of the multilayers were also determined. Multilayers with higher-hardness have higher values of Young's modulus. The values of Young's modulus are by approx. 2 times greater than the Young's moduli for solid copper and nickel alloys.

#### 4. Summary

The study has shown a relationship between the thickness of Cu and Ni sublayers in the multilayers and their texture, roughness and mechanical properties. It has been demonstrated that Cu/Ni multilayers with a strong texture have higher surface roughness. A strong texture was characteristic of those multilayers whose variation in sublayer thickness was

greater by over two times. It has also been shown that the mechanical properties of the multilayers depend on their total thickness. The multilayers with the largest thickness have higher hardness and Young's modulus.

In conclusion, it can be stated that the properties of Cu/Ni multilayers depend both on the thickness of their sublayers, as well as on their total thickness.

#### References

- [1] KANAK J., STOBIECKI T., THOMAS A., SCHMALHORST J., REISS G., *Vacuum*, 82 (2008), 1057.
- [2] GERRIT VAN DER LAAN, *Curr. Opin. Solid. ST. M.*, 10 (2006), 120.
- [3] BARSHILIA H.C., RAJAM K.S., *Surf. Coat. Tech.*, 155 (2002), 195.
- [4] LIU Y, BUORD D., WANG H., SUN C., HANG X., *Acta Mat.*, 59 (2011), 1924.
- [5] JANG B.K., MATSUBARA H., *Mater.Lett.*, 59 (2005), 3462.
- [6] PLATT C.L., WIERMAN K.W., *J. Magn. Magn. Mater.*, 295 (2005), 241.
- [7] KUCHARSKA B., KULEJ E., WITKOWSKA M., NITKIEWICZ Z., *Inżynieria Materiałowa*, 3 (2010), 439.
- [8] KUCHARSKA B., KULEJ E., KANAK J., *Opt. Appl.*, 39, (2009), 881.
- [9] KULEJ E., KUCHARSKA B., PYKA G., GWOŹDZIK M., *Cent. Eur. J. Phys.*, 9(6) (2011), 1421.
- [10] DUŚ-SITEK M., NABIALEK M., GAĞOROWSKA B., *Opt. Appl.*, 39 (2009), 645.
- [11] GAĞOROWSKA B., DUŚ-SITEK M., NABIALEK M., *Opt. Appl.*, 39 (2009), 839.
- [12] MALZBENDER J., *J. Eur. Ceram. Soc.*, 23 (2003), 1355.
- [13] OLIVER W.C., PHARR G.M., *J. Mater. Res.*, 7 (1992), 1564.

Received: 2012-10-30

Accepted: 2012-12-09